

## Fatigue crack growth reconstitution in the specimen representing longitudinal joint of an integral panel

ŠEDEK Jakub<sup>1,a</sup> and MICHALCOVÁ Lenka<sup>1,b</sup>

<sup>1</sup>Czech Aerospace Research Centre (VZLÚ), Beranových 130, 19905, Prague, Czech Republic

<sup>a</sup>sedek@vzlu.cz, <sup>b</sup>michalcova@vzlu.cz

**Keywords:** Aluminium alloy, Crack growth, Fatigue, Reconstitution, SEM

**Abstract.** The fatigue crack growth reconstitution is presented on the crack developed in the specimen representing longitudinal joint of an integral panel. The fractographic observation was carried out using optical and scanning electron microscopy (SEM). The major crack was investigated in detail. The striation spacing was determined from several locations and processed to obtain its average values. The approach assuming the relation between the striation spacing and the crack growth rate was employed. The integral method to obtain the crack growth curve was realized. The crack growth determined by fractographic reconstitution was faster by 22% of the fatigue life. The result is on the conservative side from the point of view of safety.

### Introduction

The joint is the critical point of the structure from the aspect of strength and fatigue. The life of the component then depends on the crack initiation and growth periods. Fatigue cracks can initiate not only from the connecting elements, but also from other locations. The contact of connected parts is sometimes serious from the point of crack initiation by fretting.

The joint of the integral panel and the flange of the spar in the wing structure of a commuter airplane was tested in Czech Aerospace Research Centre in order to determine S-N curves and to monitor the crack growth. The cracks were expected to initiate at the riveted joint but in some cases the crack initiated elsewhere and determined the fatigue life of the specimen. Apparently, the fretting damage was the reason for such crack initiation as shown in Fig. 1. Due to unexpected crack initiation position, the crack growth was not monitored as the cracks initiating from the rivet hole. Therefore, the crack reconstitution by means of fractography was carried out on one specimen to show possibilities of the method.

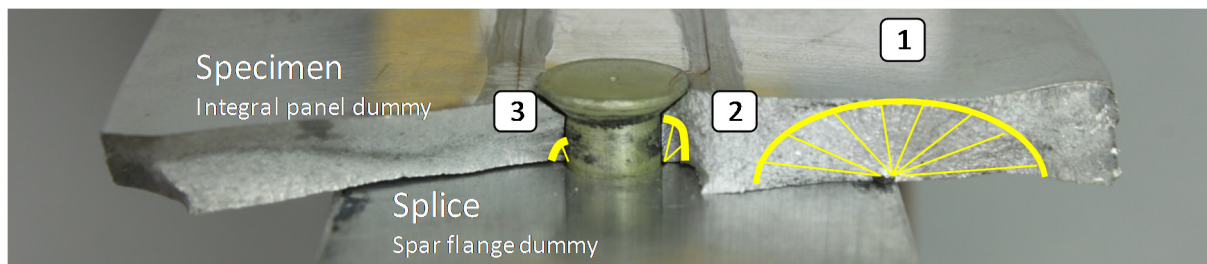


Fig. 1: Fatigue cracks in the specimen; yellow colour marks the visually visible crack fronts

**Specimen and test description.** Specimens represented the longitudinal joint of the integral wing panel and the spar flange of a commuter airplane. The specimens were made from two

components as shown in Fig. 2. One of 4.5 mm thick flat part representing the integral panel made of aluminium alloy 7475-T7351 and the splice representing the flange of 7.5 mm thick made of aluminium alloy 2124-T851. The joint was realized by rivets 5 mm in diameter with countersunk head.

Specimens were subjected to constant amplitude cyclic loading and with cycle asymmetry  $R = 0.05$ . Analysed specimen was loaded at the cycle upper level of 67 MPa for 5 000 000 cycles and then the load level was increased up to 220 MPa. The failure subsequently occurred after 5 878 cycles.

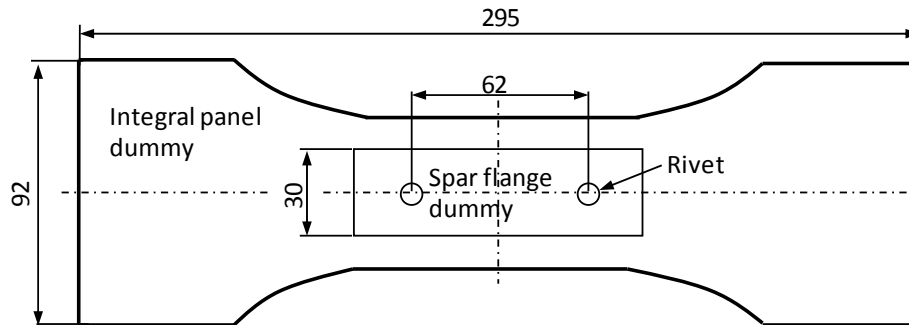


Fig. 2: Specimen representing the longitudinal joint of integral wing panel and the spar flange; dimensions in mm

**Fractographic observation of crack surfaces.** The visual inspection of fracture surfaces was carried out primarily using optical microscopy. The major crack was observed on the cracked surfaces and the initiation point was easily identified due to clear radial steps emanating from one point and due to the clearly visible border between two regions, obviously different from the point of view of micromorphology. The initiation spot was located at the contact with the splice. Due to the different stiffness of connected parts, relative displacements were present and fretting occurred. At the crack initiation, the flaw was  $0.36 \times 1$  mm in size. The crack development was regular to all directions according to beach mark on the surface.

Minor cracks were located opposite each other at the edge of the rivet hole adjacent to the splice. The initiation of the minor cracks marked as no. 2 and no. 3 started from the grooves made by the drill tool and from the rough surface inside the hole. The microcracks linked together formed the corner crack. Their development was slower than the major crack and so they remained only quarter-circle shaped at the time of the final failure.

The surface of major crack was analysed in more detail by means of scanning electron microscopy (SEM) using TESCAN VEGA apparatus. The analysed crack is marked as crack no. 1 in Fig. 1.

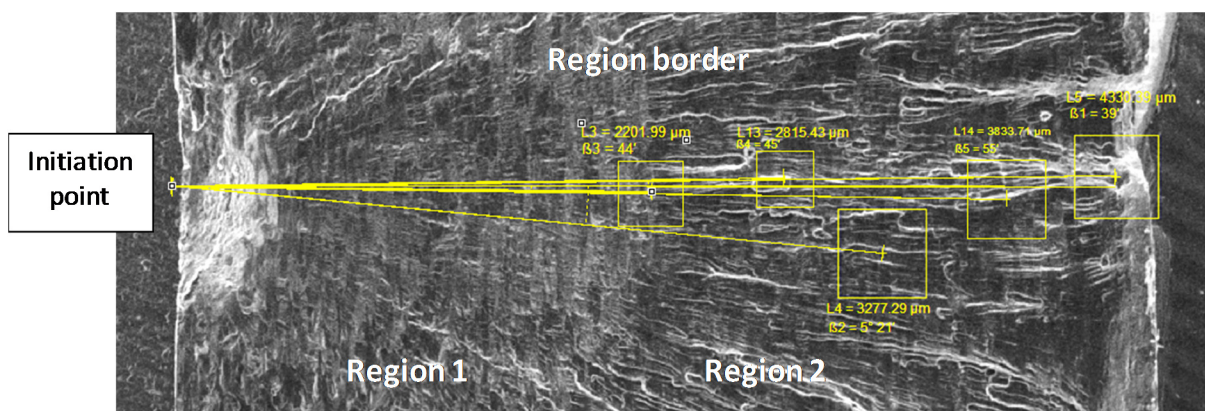


Fig. 3: SEM picture of the major crack; rectangles mark inspected locations in more detail

The beach mark distinguishing fracture surface into two regions is the significant attribute of the crack no. 1. The regions are marked in Fig. 3. The region border is the half circle shaped reaching up to half of the thickness. Different micromorphology in the regions can be attributed to the crack growth under different loading conditions before and after the change of the load level. The focus for SEM was given to the region 2, where the striations were expected. In the region 1, the striations were very difficult to observe.

**Fractographic reconstitution of crack growth.** Based on the work [1] the fractographic reconstitution of crack growth in region 2 was realized. The quantitative fractographic data based on striation spacing are necessary to determine from several locations by means of SEM. Five locations were chosen for a more detailed analysis (see Fig. 3). In each location, several measurements of the series of striations were carried out. The average striation spacing  $s_{ij}$  in the direction of macrocrack growth and the average angle  $\vartheta_{ij}$  of local and global crack growth is the result from each location. Micromorphology pictures were evaluated at the crack lengths of 2.20, 2.82, 3.27, 3.83 and 4.43 mm. The results are stated in Tab. 1 and the example of the local processing at length of 4.43mm is shown in Fig. 4.

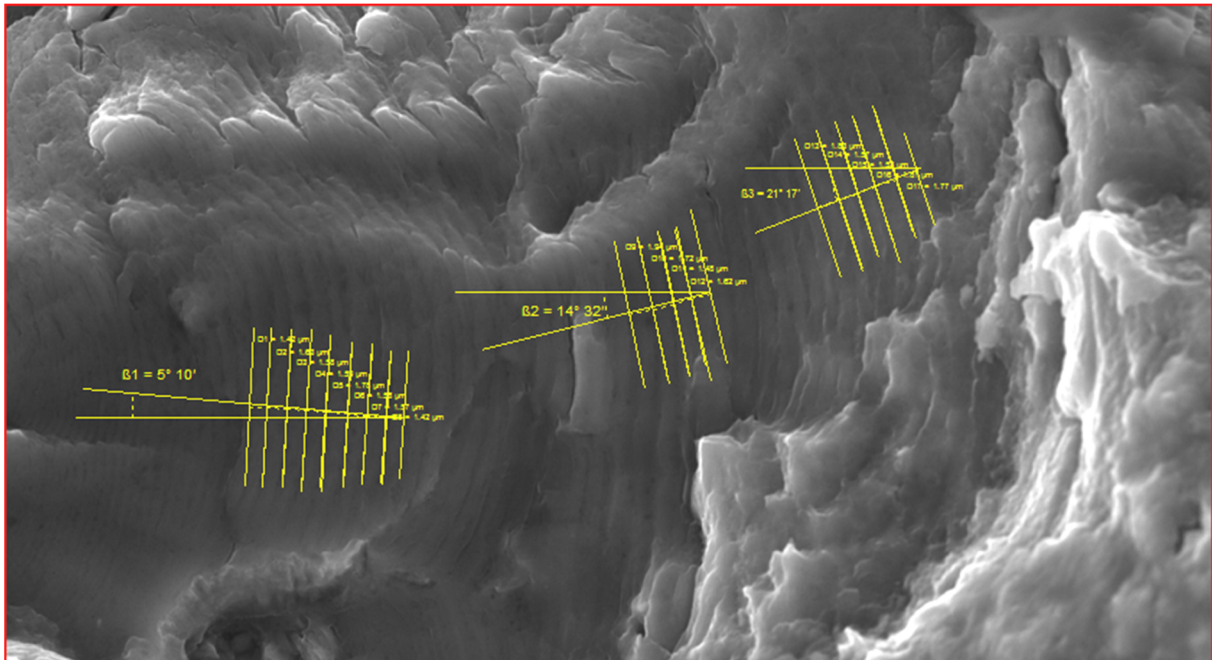


Fig. 4: SEM picture of the major crack detail at distance of 4.43 mm from the initiation point; Parallel lines mark the striation fronts and wedges represents the inclination of the global and local crack growth.

The SEM pictures  $ij$  do not lie on the same line and the crack front is also curved, so the striation spacing in the global direction of crack growth  $s_{ij}^g$  was also determined.

Tab. 1: Basic micromorphological characteristics from analysed locations in region 2 of the crack n. 1.

Distance from the initiation point (mm)	2.201	2.815	3.269	3.834	4.320
$s_{ij}$ ( $\mu\text{m}$ )	0.37	0.32	0.58	0.62	1.64
$\vartheta_{ij}$ (rad)	0	-0.04	0.07	0.49	0.12
$s_{ij}^g$ ( $\mu\text{m}$ )	0.36	0.33	0.58	0.55	1.61

The average striation spacing  $s_{ij}^g$  (thereinafter denoted as  $s$ ) in dependence on the crack length  $a$  was fitted by equation

$$s = 1.41 E - 06 \cdot \exp(a/0.637) + 0.234 E - 03 \quad (1)$$

The relationship  $s=s(a)$  is used for the reconstitution of crack kinetics utilizing the dependency of crack length  $a$  on the elapsed cycles  $N$ . The number of elapsed cycles  $N_x$  at corresponding crack length  $a_x$  was determined according to

$$N_x = \int_{a_1}^{a_x} \frac{da}{D(s) \cdot s(a)} + N_i \quad (2)$$

where the parameter  $D$  denotes the relation between striation spacing and the macroscopic crack growth  $v = da/dN$  and is dependent on several variables; e.g. material, its heat treatment, or loading conditions. Generally,  $D$  requires to be determined experimentally.  $N_i$  is the initial cycle number and  $a_1$  denotes initial crack length. Parameter  $D$  can be expressed for the correlation of macroscopic and microscopic characteristics as  $D=v/s$ .

Influence of loading conditions is being described by the dependency on the stress intensity factor  $K_{eff}$ . For the aluminium alloy 7475-T7351, the match of crack growth rate  $da/dN$  and the striation spacing  $s$  was found for the cycle asymmetry  $R = 0.1$  and  $v$  in the range  $0.18 - 2.02 \mu\text{m}/\text{cycle}$  [2]. The coefficient  $D = 1$  was assumed for presented work also for  $R = 0.05$  and the whole range of  $\Delta K$ .

Integrating Eq. (2) from  $a_i$  up to  $a_x$  the number of cycles can be obtained. Substituting the Eq. (1) into Eq. (2) the direct formula was achieved according to [3]

$$N_x = \frac{a_x - a_i}{C} + \frac{1}{BC} \ln \left| \frac{C + A \exp(Ba_i)}{C + A \exp(Ba_x)} \right| + N_i \quad (3)$$

where using constants  $A = 1.41 E-06$ ,  $B = 1/0.637$  and  $C = 0.234 E-03$ . The result of crack growth curve is shown in Fig. 6. In comparison with experimental data, the reconstituted number of cycles up to the failure in crack growth region 2 is less by 22%.

**Reconstitution of the crack growth by methods of fracture mechanics.** The crack growth curve was independently determined also by the simulation of crack growth, because the crack growth data was not available from the test. The elapsed cycles at load level change up to 220 MPa and the specimen failure at 5878 cycles were only available data. The beach mark distinguishing between region 1 and region 2 was attributed to the load level change. From the fractographic analysis the shape of the crack front at this point is known and with material crack growth data the simulation could be performed.

The AFGROW code [4] was utilized for the crack growth simulation. The shape function of the surface crack implemented in the code was used for the calculation of stress intensity factor  $K$ . The model represented only one half of the specimen due to lack of the model including the hole. Representative solution can be assumed up to reaching the whole thickness of the specimen by the crack. Substitutive model dimensions are shown in Fig. 5.

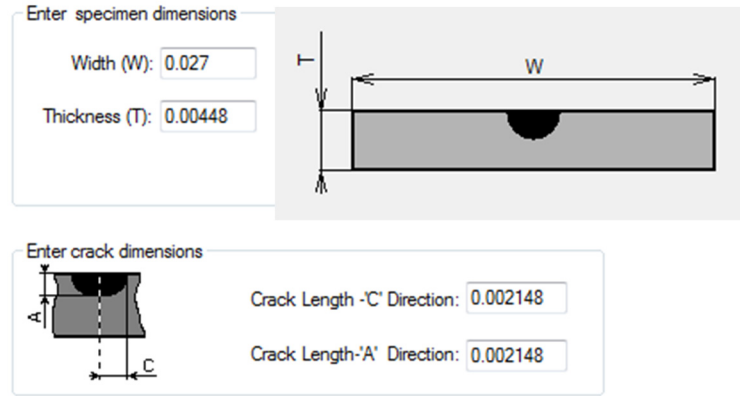


Fig. 5: Crack growth curve obtained by fractographic reconstitution in region 2 of fracture surface.

Material characteristics are used according to Ref. [5] in the form of the relationship of  $da/dN$  versus  $\Delta K$  for load asymmetry  $R = 0.02$  described by the linear formula. Crack growth rate was computed according to Paris law [6]

$$\frac{da}{dN} = C\Delta K^m \quad (4)$$

where  $C = 1.816 \text{ E-}10$  and  $m = 2.814$ . Characteristics determined at load ratio  $R = 0.02$  are assumed not to be significantly different from those determined at  $R = 0.05$  and are used for the simulation. Crack growth increments are integrated from the crack length of 2.15 mm up to 4.5 mm. The results of simulation in comparison with the fractographic reconstitution are shown in Fig. 6.

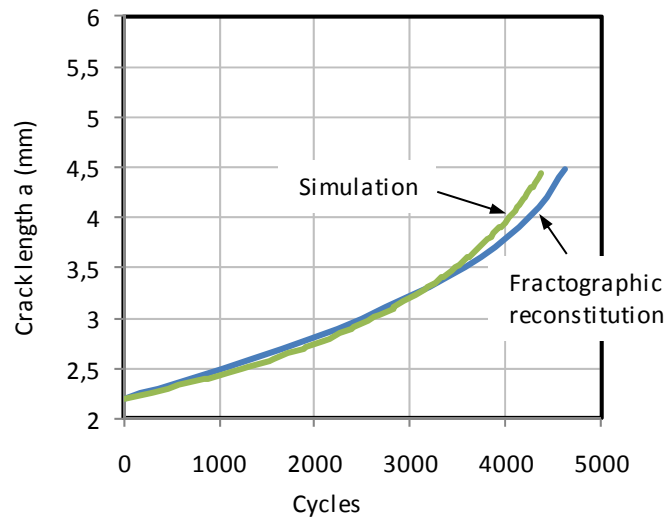


Fig. 6: Crack growth curve determined by the simulation in comparison with the curve determined by fractographic reconstitution in region 2 of fracture surface.

## Conclusions

Fatigue crack growth reconstitution in the specimen representing the longitudinal joint of integral panel was performed. Fractographic analysis was employed to determine the striation spacing in several locations of the cracked surface. The integral method to obtain the crack growth curve was realized. The crack growth determined by the fractographic reconstitution is

faster by 22% of final life. The results were also compared with the simulated crack growth curve showing good match of both curves with slight deviation at the last 20% of the specimen life. The result is on the conservative side from the point of view of safety.

### **Acknowledgments**

This project result was developed within the institutional support of the Ministry of Industry and Trade of the CR directed to the development of research organizations.

### **References**

- [1] Nedbal J. et al. Fractographic Reconstitution of Fatigue Crack History – Part I. Fatigue and Fracture of Engineering Materials and Structures, 31 (2), 2008. pp.164-176. doi: 10.1111/j.1460-2695.2007.01211.x
- [2] Ruckert C.O.F.T. et al. On the Relation Between Micro- and Macroscopic Fatigue Crack Growth Rates in Aluminum Alloy AMS 7475-T7351
- [3] Rektorys K et al. Přehled užité matematiky. 3. vydání, SNTL, Praha, 1973.
- [4] Harter J.A. AFGROW Users' Guide and Technical Manual, Air Force Research Laboratory, 1999. AFRL-VA-WP-1999-3016
- [5] Homola et al. Materiálové charakteristiky desky tl. 76 mm vyrobené ze slitiny 7475-T7351 ve směru L-T (Alcoa), VZLÚ, 2013. R-5650
- [6] P.C. Paris and F. Erdogan. A critical Analysis of Crack Propagation Laws, Journal of Basic Engineering, 85 (4), 1963. pp. 528-533, doi:10.1115/1.3656900